η photoproduction of nucleons and the structure of the resonance $S_{11}(1535)$ in the quark model

Zhenping Li

Physics Department, Carnegie-Mellon University, Pittsburgh, Pennsylvania 15213-3890

In this paper, we present our study on η photoproduction based on the chiral quark model. We find that the quark model provides a very good description of η production with far fewer parameters, and the threshold region is not a reliable source to determine the ηNN coupling constant due to its strong dependence on the properties of the resonance $S_{11}(1535)$. We suggest that the systematic data in $E_{\text{lab}} = 1.2 - 1.4$ GeV region may help us to determine the ηNN coupling constant more precisely. The structure of the resonance $S_{11}(1535)$ is discussed; we find that the recent data from Mainz group bring the helicity amplitude much closer to the quark model prediction. However, more studies need to be done to understand the large ηN branching ratio of the resonance $S_{11}(1535)$. Our results show that the quark model is a very good approach to studying the underlying structure of baryon resonances from the meson photoproduction data.

I. INTRODUCTION

In our previous publication [1], a framework based on the chiral quark model to study meson photoproduction was developed. It started from the low energy QCD Lagrangian [2] so that the meson-quark interaction was chiral invariant and the low energy theorem in the threshold pion photoproduction [3] was automatically recovered [4] with a proper treatment of the center of mass motion [5]. By treating the pseudoscalar mesons as Goldstone bosons that interact directly with quarks inside baryons, the quark model provides a unified formalism for all s- and u-channel resonances, and the number of parameters used in the model is dramatically reduced. In principle, only one parameter is needed for all resonances that contribute to the meson productions. This marks a significant advance from the traditional theory, in which effective couplings among the hadrons are used so that each resonance requires one additional parameter. It also makes it possible to provide a consistent calculation of meson photoproduction beyond the threshold region. Perhaps, more importantly, it provides a unified description for pseudoscalar meson photoproduction and highlights the dynamic role of baryon resonances in each process. In this paper, we extend our investigation to η photoproduction.

There are many features of η mesons that make η photoproduction unique in the quark model. The η meson is an isospin zero state; thus, only the resonances with isospin 1/2 contribute in the s and u channels. It is also a charge neutral particle so that the contact (seagull) term [1] that plays a dominant role in charge meson production does not contribute and, thus, enhances the role of resonances. Moreover, because the mass of the resonance $S_{11}(1535)$ is just above the ηN threshold where the S wave is dominant, η photoproduction in the threshold region provides a very important probe of the structure of the resonance $S_{11}(1535)$. Thus there has

been considerable theoretical and experimental interest in studying η photoproduction. New experimental data for η photoproduction in the threshold region from Bates [6], the Bonn accelerator ELSA [7], and Mainz [8] have been published recently. In particular, data from the Mainz group provide a more systematic behavior of η production in the threshold region, which has better energy and angular resolutions, thus enabling us to study the properties of the resonance $S_{11}(1535)$ more precisely. Therefore, it is very interesting to note that the helicity amplitude $A^p_{1/2}$ extracted from the new Mainz data [8] is much closer to the prediction of the quark model [9,10]. On the theoretical side, theoretical studies of η photoproduction have been mostly in the framework of Breit-Wigner parametrizations [11] or coupled channel isobar models [12]. The recent investigation by the RPI group [13] has made significant progress in this field, in which the effective Lagrangian approach is used so that the properties of the resonance $S_{11}(1535)$ extracted from the data are more model independent and the number of parameters is reduced considerably.

Traditionally, investigations of meson photoproduction in the framework of the quark model have concentrated on the transition amplitudes, in particular the helicity amplitudes for the electromagnetic transitions and the partial wave amplitudes for the mesonic decays of baryon resonances. These amplitudes were extracted from meson photoproduction data by phenomenological models; thus, they are less model independent. Instead of relying on the transition amplitudes from the phenomenological models, the quark model approach enables us to study the structure of baryon resonances directly from the photoproduction data. Thus a connection between meson photoproduction and more fundamental theories based on QCD can be established. Because the transition amplitudes in the quark model have very different energy and momentum dependences from those in traditional models, it is by no means trivial if meson photoproduc-

tion can be successfully described by the quark model. This requires that the transition amplitudes in the model have correct off-shell behavior, which are usually evaluated on shell. Our early investigation [1] in kaon photoproduction has shown that the quark model approach presents a much better framework to understand the reaction mechanism of meson photoproduction than many traditional hadronic models, and we shall show that the results in η photoproduction are equally encouraging.

The paper is organized as follows. The general formalism in the quark model for η photoproduction is presented in Sec. II. We have carried out three different calculations in Sec. III: The first assumes $SU(6) \otimes O(3)$ symmetry for the baryon wave functions so that only one parameter is required to fit the experimental data; the second includes possible configuration mixing effects for the resonances $S_{11}(1535)$ and $S_{11}(1650)$ with three additional parameters; and the third calculation is concentrated on fitting the recent Mainz data to extract properties of the resonance $S_{11}(1535)$. Because the data from Mainz group are significantly different from the rest, we fit them separately. In Sec. IV, we discuss the structure of the resonance $S_{11}(1535)$ from the η photoproduction data in the threshold region and highlight the problems yet to be resolved. Finally, the conclusions are given in Sec. V.

II. GENERAL FORMALISM

There are two major components in addition to the calculation of the electromagnetic and strong transitions of the baryon resonances in the quark model approach, which has been shown to be crucial in deriving the model-independent low energy theorem in threshold pion photoproduction [4]. First, one has to combine the phenomenological quark model with chiral symmetry, this is being achieved by the introduction of the chiral QCD Lagrangian [2] so that the meson transition operators are chiral invariant. Second, since a baryon is being treated as a three-quark system, the separation of the center of mass motion from the internal motion is important to recover the low energy theorem in threshold pion photoproduction; this has been discussed in detail for Compton scattering $\gamma N \rightarrow \gamma N$ [5].

The differential cross section in the center-of-mass frame is

$$\frac{d\sigma^{\text{c.m.}}}{d\Omega} = \frac{\alpha_e \alpha_\eta (E^i + M_N)(E^f + M_N)}{16 s M_N^2} \frac{|\mathbf{q}|}{|\mathbf{k}|} |\mathcal{M}_{fi}|^2 , \quad (1)$$

where α_η is the ηNN coupling constant, α_e is the electromagnetic coupling, and $\sqrt{s} = E^i + \omega_\gamma = E^f + \omega_\eta$ is the total energy in the c.m. frame. Generally, the η transitions between the resonances and the nucleon can be expressed in terms of the α_η, and no additional parameter for each resonance is required.

Therefore, the coupling constant has been removed from the matrix element $\mathcal{M}_{fi}$ so that it becomes dimensionless. The coupling constant α_η is treated as a free parameter because of the theoretical issues, such as the $U(1)$ anomaly, and η-η' mixing.

One can write the matrix element $\mathcal{M}_{fi}$ in terms of the Chew-Goldberger-Low-Nambo (CGLN) [3] amplitudes:

$$\mathcal{M}_{fi} = \mathbf{J} \cdot \boldsymbol{\epsilon} , \quad (2)$$

where $\boldsymbol{\epsilon}$ is the polarization vector and the current J is written as

$$\mathbf{J} = f_1 \boldsymbol{\sigma} + i f_2 \frac{(\boldsymbol{\sigma} \cdot \mathbf{q})(\mathbf{k} \times \boldsymbol{\sigma})}{|\mathbf{q}||\mathbf{k}|} + f_3 \frac{\boldsymbol{\sigma} \cdot \mathbf{k}}{|\mathbf{q}||\mathbf{k}|} \mathbf{q} + f_4 \frac{\boldsymbol{\sigma} \cdot \mathbf{q}}{\mathbf{q}^2} \mathbf{q}$$

$$(3)$$

in the center-of-mass frame. The differential cross section in terms of the CGLN amplitude is [14]

$$|\mathcal{M}_{fi}|^2 = \text{Re} \Bigg\{ |f_1|^2 + |f_2|^2 - 2\cos(\theta) f_2 f_1^*$$

$$+ \frac{\sin^2(\theta)}{2} [|f_3|^2 + |f_4|^2 + 2 f_4 f_1^* + 2 f_3 f_2^*$$

$$+ 2\cos(\theta) f_4 f_3^*] \Bigg\} , \quad (4)$$

where θ is the angle between the incoming photon momentum $\mathbf{k}$ and outgoing η momentum $\mathbf{q}$ in the center of mass frame. The various polarization observables can also be expressed in terms of CGLN amplitudes, which can be found in Ref. [14].

The electromagnetic coupling in the nonrelativistic limit is [1]

$$h_e = \sum_j e_j \left[r_j \cdot \boldsymbol{\epsilon} \left(1 - \frac{\mathbf{p}_j \cdot \mathbf{k}}{m_q \omega_\gamma} \right) - \frac{1}{2m_q} \boldsymbol{\sigma}_j \cdot (\boldsymbol{\epsilon} \times \mathbf{k}) \right] , \quad (5)$$

and it has been shown [4] that the operator h_e in Eq. (5) is sufficient to reproduce the low energy theorem for threshold pion photoproduction [3]. The corresponding η transition operator is a pseudovector coupling:

$$H_\eta^{\text{nr}} = \sum_j \boldsymbol{\sigma}_j \cdot \left[\mathbf{A} + \frac{2\omega_\eta}{m_q} \mathbf{p}_j \right] , \quad (6)$$

where $\mathbf{A}$ corresponds to the center of mass motion and depends on the momenta of the initial and final states, and $\mathbf{p}_j$ is the internal momentum for a three-quark system.

Because the η meson is a charge neutral particle, the seagull term that plays an important role in charge meson production does not contribute. Thus the leading Born term would be the nucleon pole term in the S and U channels:

$$\mathcal{M}_S = \omega_\eta e^{-(\mathbf{q}^2 + \mathbf{k}^2)/6\alpha^2} \left(\frac{1}{E^f + M_N} + \frac{1}{E^i + M_N} \right) \left(1 - \frac{\mathbf{k}^2}{4P^i \cdot k} \mu_N \right) \boldsymbol{\sigma} \cdot \boldsymbol{\epsilon}$$

$$+ i e^{-(\mathbf{k}^2 + \mathbf{q}^2)/6\alpha^2} \left[\frac{\omega_\eta}{2} \left(\frac{1}{E^f + M_N} + \frac{1}{E^i + M_N} \right) + 1 \right] \frac{\mu_N}{2P^i \cdot k} \boldsymbol{\sigma} \cdot \mathbf{q} \boldsymbol{\sigma} \cdot (\boldsymbol{\epsilon} \times \mathbf{k}) , \quad (7)$$

where $P^f \cdot k = \omega_\gamma(E^i + \omega_\gamma)$, μ_N is the magnetic moments of the nucleon, and α^2 is the constant from the harmonic oscillator wave functions. The matrix element for the U-channel nucleon exchange term is

$$\mathcal{M}_U = -e^{-(\mathbf{k}^2+\mathbf{q}^2)/6\alpha^2} \frac{\mu_N}{2P^f \cdot k} \left\{ \frac{\omega_\eta \mathbf{k}^2}{2} \left(\frac{1}{E^f + M_N} + \frac{1}{E^i + M_N} \right) \sigma \cdot \epsilon \right.$$
$$\left. +i \left[\frac{\omega_\eta}{2} \left(\frac{1}{E^f + M_N} + \frac{1}{E^i + M_N} \right) + 1 \right] \sigma \cdot (\epsilon \times \mathbf{k}) \sigma \cdot \mathbf{q} \right\} , \tag{8}$$

where $P^f \cdot k = \omega_\gamma(E^f + |\mathbf{q}| \cos\theta)$.

The contributions from the t-channel exchange are not included in this approach. This has been discussed in some detail in the literature [15]; if a complete set of resonances is introduced in the s and u channels, the inclusion of the t-channel exchange might lead to a double counting problem. This may turn out to be an advantage of the quark model approach, since fewer free parameters are needed to fit the data.

The first excited resonance that contributes to η production is the Roper resonance $P_{11}(1440)$. In the SU(6) quark model, its U-channel contribution is

$$\mathcal{M}_{P_{11}(1440)} = \frac{-M_{P_{11}(1440)} \mathbf{k}^2 e^{-(\mathbf{q}^2+\mathbf{k}^2)/6\alpha^2}}{(P^f \cdot k + \delta M_{P_{11}(1440)}^2/2)216 m_q \alpha^2} \left\{ \frac{\omega_\eta \mathbf{k}^2 \mathbf{q}^2}{\alpha^2} \left[\frac{1}{E^i + M_N} \right. \right.$$
$$\left. \left. + \frac{1}{E^f + M_N} \right\} \sigma \cdot \epsilon - i \left\{ \frac{\omega_\eta}{\mu_q} - \left[\frac{\omega_\eta}{E^f + M_N} + 1 \right] \frac{\mathbf{q}^2}{\alpha^2} \right\} \sigma \cdot (\epsilon \times \mathbf{k}) \sigma \cdot \mathbf{q} \right\}, \tag{9}$$

where $\delta M_{P_{11}(1440)}^2 = M_{P_{11}(1440)}^2 - M_N^2$, and its S-channel contribution will be given later.

For the excited resonance with higher energy, such as P-wave baryons, we could treat them as degenerate, since their contributions in the U channel are much less sensitive to the detailed structure of their masses than those in the S channel. Therefore, we can write their U-channel contributions in a compact form:

$$\mathcal{M}_U = (\mathcal{M}_U^3 + \mathcal{M}_U^2) e^{-(\mathbf{k}^2+\mathbf{q}^2)/6\alpha^2} . \tag{10}$$

The first term in Eq. (10) represents the process in which the incoming photon and outgoing η meson are absorbed and emitted by the same quarks; it is

$$\mathcal{M}^3 = \frac{1}{2m_q} \{ i\mathbf{A} \cdot (\epsilon \times \mathbf{k}) + \sigma \cdot [\mathbf{A} \times (\epsilon \times \mathbf{k})] \} F \left(\frac{\mathbf{k} \cdot \mathbf{q}}{3\alpha^2}, P^f \cdot k \right)$$
$$+ \frac{1}{3} \left[\frac{\omega_\eta \omega_\gamma}{m_q} \left(1 + \frac{\omega_\gamma}{2m_q} \right) \sigma \cdot \epsilon + \frac{\omega_\gamma}{\alpha^2} \sigma \cdot \mathbf{A} \epsilon \cdot \mathbf{q} \right] F \left(\frac{\mathbf{k} \cdot \mathbf{q}}{3\alpha^2}, P^f \cdot k + \delta M^2 \right)$$
$$+ \frac{\omega_\eta \omega_\gamma}{9\alpha^2 m_q} \sigma \cdot \mathbf{k} \epsilon \cdot \mathbf{q} F \left(\frac{\mathbf{k} \cdot \mathbf{q}}{3\alpha^2}, P^f \cdot k + 2\delta M^2 \right) , \tag{11}$$

where

$$\mathbf{A} = -\omega_\eta \left(\frac{1}{E^i + M_N} + \frac{1}{E^f + M_N} \right) \mathbf{k} - \left(\omega_\eta \frac{1}{E^f + M_N} + 1 \right) \mathbf{q} . \tag{12}$$

The function $F(x, y)$ in Eq. (11) corresponds to the product of the spatial integral and the propagator for the excited states; it can be written as

$$F(x, y) = \sum_n \frac{M_n}{n!(y + n\delta M^2)} x^n , \tag{13}$$

where $n\delta M^2 = (M_n^2 - M^2)/2$ represents the mass difference between the ground state and excited states with the major quantum number n in the harmonic oscillator basis, which will be chosen as the average mass difference between the ground state and the negative parity baryons so that $\delta M^2 \approx 0.74$ GeV^2. The first term in Eq. (11) corresponds to the correlation between the magnetic transition and the c.m. motion of the η transition operator; it contributes to the leading Born terms in the U channel. The second term in Eq. (11) is the correlations among the internal and c.m. motions of the photon and η transition operators; this term only contributes to the transitions between the ground and $n \geq 1$ excited states in the harmonic oscillator basis. The third term in Eq. (11) corresponds to the correlation of the internal motions between the phonon and η transition operators, which only contributes to the transition between the ground and $n \geq 2$ excited states. The second term $\mathcal{M}_U^2$ in Eq. (10) represents the process in which the incoming photon and outgoing η are absorbed and emitted by different quarks, and we found that

$$\mathcal{M}_U^2 = 0 \ . \tag{14}$$

This is a direct consequence of isospin couplings. Equation (11) can be summed up to any quantum number n; however, the excited states with large quantum number n become less significant for the U-channel resonance contributions. Thus we only include the excited states with $n \leq 2$, which is the minimum number required for the contribution from every term in Eq. (11).

For the S-channel resonance processes, the operator $\mathbf{A}$ in Eq. (6) should be

$$\mathbf{A} = -\left(\omega_\eta \frac{1}{E^f + M_N} + 1\right)\mathbf{q} \tag{15}$$

in the c.m. frame. The calculation of the S-channel resonance contributions is similar to that of the U-channel resonance contributions. However, since the operator $\mathbf{A}$ is only proportional to the final state momentum $\mathbf{q}$, the partial wave analysis can be easily carried out for the S-channel resonances.

In general, one can write the S-channel resonance amplitudes as

$$\mathcal{M}_R = \frac{2M_R}{s - M_R^2} e^{-(\mathbf{k}^2 + \mathbf{q}^2)/6\alpha^2} \mathcal{O}_R \ , \tag{16}$$

where $\sqrt{s} = E^i + \omega_\gamma = E^f + \omega_\eta$ is the total energy of the system and $\mathcal{O}_R$ is determined by the structure of each resonance. Equation (16) shows that there should be a form factor $e^{-(\mathbf{k}^2 + \mathbf{q}^2)/6\alpha^2}$ in the harmonic oscillator basis, even in the real photon limit. If the mass of a resonance is above the threshold, the mass M_R in Eq. (16) should be changed to

$$M_R^2 \to M_R[M_R - i\Gamma(\mathbf{q})] \ . \tag{17}$$

$\Gamma(\mathbf{q})$ in Eq. (17) is the total width of the resonance and a function of the final state momentum $\mathbf{q}$. For a resonance decay to a two-body final state with orbital angular momentum l, the decay width $\Gamma(\mathbf{q})$ can be written as

$$\Gamma(\mathbf{q}) = \Gamma_R \frac{\sqrt{s}}{M_R} \sum_i x_i \left(\frac{|\mathbf{q}_i|}{|\mathbf{q}_i^R|}\right)^{2l+1} \frac{D_l(\mathbf{q}_i)}{D_l(\mathbf{q}_i^R)} \ , \tag{18}$$

with

$$|\mathbf{q}_i^R| = \sqrt{\frac{(M_R^2 - M_N^2 + M_i^2)^2}{4M_R^2} - M_i^2} \tag{19}$$

and

$$|\mathbf{q}_i| = \sqrt{\frac{(s - M_N^2 + M_i^2)^2}{4s} - M_i^2} \ , \tag{20}$$

where x_i is the branching ratio of the resonance decaying into a meson with mass M_i and a nucleon, and Γ_R is the total decay width of the S-channel resonance with mass M_R. The function $D_l(\mathbf{q})$ in Eq. (18) is called the fission barrier [16] and is wave function dependent; here, we use

$$D_l(\mathbf{q}) = \exp\left(-\frac{\mathbf{q}^2}{3\alpha^2}\right) \ , \tag{21}$$

which is independent of l. A similar formula used in $I = 1$ $\pi\pi$ and p-wave $I = 1/2$ $K\pi$ scattering was found in excellent agreement with data in the ρ and K^* meson region [17]. Generally, the resonance decays are dominated by the pion channels, except the resonance $S_{11}(1535)$ whose branching ratio of ηN channels is around 50%. Therefore, we simply set $x_\pi = x_\eta = 0.5$ for the resonance $S_{11}(1535)$, while $x_\pi = 1.0$ for the rest of the resonances as a first-order approximation.

The operator $\mathcal{O}_R$ in Eq. (16) can be generally written as

$$\begin{aligned}\mathcal{O}_R = A[&f_1^R \boldsymbol{\sigma} \cdot \boldsymbol{\epsilon} + if_2^R(\boldsymbol{\sigma} \cdot \mathbf{q})\boldsymbol{\sigma} \cdot (\mathbf{k} \times \boldsymbol{\epsilon}) \\ &+ f_3^R \boldsymbol{\sigma} \cdot \mathbf{k}\boldsymbol{\epsilon} \cdot \mathbf{q} + f_4^R \boldsymbol{\sigma} \cdot \mathbf{q}\boldsymbol{\epsilon} \cdot \mathbf{q}]\end{aligned} \tag{22}$$

for pseudoscalar meson photoproduction, where A is the meson decay amplitude and f_i^R ($i = 1, ..., 4$) is the photon transition amplitude. The meson decay amplitude A is determined by the spatial wave function of resonances and the relative angular momentum between the final decay products. In Table I, we present the amplitude A in the simple harmonic oscillator basis, in which the amplitude A depends on the total excitation n and the orbital angular momentum L. The relative angular momentum of the final decay products is expressed in terms of partial wave language in Table I, in which the S, P, D, and F waves denote the relative angular momenta 0, 1, 2, and 3 between the final decay products. The decay amplitude A in Table I is the same as the expression in Table I in Ref. [10] with $g - \frac{1}{3}h = |\mathbf{A}|/|\mathbf{q}|$, and $h = \omega_\eta/m_q$. Note that $\mathbf{A}$ has a negative sign; this is consistent with the fitted value for $g - \frac{1}{3}h$ and h in Ref. [10].

The photon transition amplitudes f_i^R in Eq. (22) are written in terms of the CGLN amplitudes, which are shown in Table II. They are usually expressed in terms of helicity amplitudes $A_{1/2}$ and $A_{3/2}$, and the connection between the two representations can be established. A very important example is the vanishing helicity amplitudes for the transitions between the resonances belonging to the $(70, ^4N)$ representation and protons due to the Moorhouse selection rule [18] if one uses the nonrelativistic transition operator in Eq. (5); consequently, the CGLN amplitudes for these resonances are zero as well. There are three important negative parity baryons that belong to the $(70, ^4N)$ multiplet in the naive quark model: $S_{11}(1650)$, $D_{13}(1700)$, and $D_{15}(1675)$. However,

TABLE I. Meson transition amplitudes A in the simple harmonic oscillator basis.

(N, L)	Partial waves	A
$(0,0)$	P	$-\left(\frac{\omega_\eta}{E^f + M_N} + 1\right)$
$(1,1)$	S	$\frac{2\omega_\eta}{m_q} - \left(\frac{\omega_\eta}{E^f + M_N} + 1\right)\frac{2\mathbf{q}^2}{3\alpha^2}$
$(1,1)$	D	$-\left(\frac{\omega_\eta}{E^f + M_N} + 1\right)$
$(2,0)$	P	$\frac{2\omega_\eta}{m_q} - \left(\frac{\omega_\eta}{E^f + M_N} + 1\right)\frac{\mathbf{q}^2}{\alpha^2}$
$(2,2)$	P	$\frac{2\omega_\eta}{m_q} - \left(\frac{\omega_\eta}{E^f + M_N} + 1\right)\frac{2\mathbf{q}^2}{5\alpha^2}$
$(2,2)$	F	$-\left(\frac{\omega_\eta}{E^f + M_N} + 1\right)\frac{\mathbf{q}^2}{\alpha^2}$

TABLE II. CGLN amplitudes for the S-channel baryons resonances for the proton target in the SU(6)⊗O(3) symmetry limit, where $k = |\mathbf{k}|$, $q = |\mathbf{q}|$, and $x = (\mathbf{k} \cdot \mathbf{q})/kq$. The CGLN amplitudes for the $N(^4P_M)$, $N(^4S_M)$, and $N(^4D_M)$ states are zero due to the Moorhouse selection rule; see text.

States	f_1	f_2	f_3	f_4
$N(^2P_M)_{\frac{1}{2}}^{-}$	$\frac{\omega_\gamma}{6}\left(1 + \frac{k}{2m_q}\right)$	0	0	0
$N(^2P_M)_{\frac{3}{2}}^{-}$	$-\frac{\omega_\gamma}{9}\left(1 + \frac{k}{2m_q}\right)\frac{q^2}{\alpha^2}$	$-\frac{kqx}{6m_q\alpha^2}$	0	$\frac{\omega_\gamma}{3\alpha^2}$
$N(^2S'_s)_{\frac{1}{2}}^{+}$	0	$-\frac{k^2}{216m_q\alpha^2}$	0	0
$N(^2D_s)_{\frac{3}{2}}^{+}$	$\frac{k^2qx}{36\alpha^2}\left(1 + \frac{k}{2m_q}\right)$	$\frac{k^2}{216m_q\alpha^2}$	$\frac{\omega_\gamma}{36\alpha^2}$	0
$N(^2D_s)_{\frac{5}{2}}^{+}$	$-\frac{k^2qx}{90\alpha^2}\left(1 + \frac{k}{2m_q}\right)$	$-\frac{k^2}{72m_q\alpha^2}\left(x^2 - \frac{1}{5}\right)$	$-\frac{k}{90\alpha^2}$	$\frac{k^2x}{18q\alpha^2}$
$N(^2S_M)_{\frac{1}{2}}^{+}$	0	$-\frac{k^2}{216m_q\alpha^2}$	0	0
$N(^2D_M)_{\frac{3}{2}}^{+}$	$\frac{k^2qx}{36\alpha^2}\left(1 + \frac{k}{2m_q}\right)$	$\frac{k^2}{216m_q\alpha^2}$	$\frac{k}{36\alpha^2}$	0
$N(^2D_M)_{\frac{5}{2}}^{+}$	$-\frac{k^2qx}{90\alpha^2}\left(1 + \frac{k}{2m_q}\right)$	$-\frac{k^2}{72m_q\alpha^2}(x^2 - \frac{1}{5})$	$-\frac{k}{90\alpha^2}$	$\frac{k^2x}{18q\alpha^2}$

it has been shown in a potential quark model calculation [19] that the two states $70N(^2P_M)_{\frac{1}{2}}^{-}$ and $70N(^4P_M)_{\frac{1}{2}}^{-}$ are strongly mixed. Therefore, the contribution from the resonance $S_{11}(1650)$ to η photoproduction will be studied by fitting to the experimental data. Indeed, this will provide us direct insight into configuration mixing in the potential quark model.

The CGLN amplitudes for the resonances with total spin 1/2 can be easily related to the helicity amplitude $A_{1/2}$ that has been frequently calculated in the quark model. Only the CGLN amplitude f_1^R is nonzero for the resonance $S_{11}(1535)$, and this corresponds to a E_0^+ multipole transition [14]. Moreover, the amplitudes f_1^R for the S-wave resonances have the same structure as the corresponding helicity amplitude $A_{1/2}$ in Ref. [26], in which the same nonrelativistic transition operator is used. For the P-wave resonances, such as the resonances $P_{11}(1440)$ and $P_{11}(1710)$, only the CGLN amplitude f_2^R is present,

which gives a M_1^- transition. Notice that the resonances with isospin 3/2 do not contribute to η photoproduction due to the isospin coupling between the η meson and the nucleon. These results provide an important consistency check for the CGLN amplitudes in Table II.

If one intends to calculate the reaction beyond 2 GeV in the center-of-mass frame, the higher resonances with quantum number $n = 3$ and $n = 4$ must be included. Instead, we adopt an approach that treats the resonances for $n \geq 3$ as degenerate; the sum of the transition amplitudes from these resonances can be obtained through the approach in Ref. [5]. The transition amplitude for the nth harmonic oscillator shell is

$$\mathcal{O}_n = \mathcal{O}_n^2 + \mathcal{O}_n^3 , \tag{23}$$

where the amplitudes $\mathcal{O}_n^2$ and $\mathcal{O}_n^3$ have the same meaning as the amplitudes $\mathcal{M}_U^2$ and $\mathcal{M}_U^3$ in Eqs. (11) and (14), and we have

$$\mathcal{O}_n^3 = -\frac{1}{2m_q}\{i\mathbf{A} \cdot (\boldsymbol{\epsilon} \times \mathbf{k}) - \boldsymbol{\sigma} \cdot [\mathbf{A} \times (\boldsymbol{\epsilon} \times \mathbf{k})]\}\frac{1}{n!}\left(\frac{\mathbf{k} \cdot \mathbf{q}}{3\alpha^2}\right)^n$$

$$+ \frac{1}{3}\left[\frac{\omega_\eta\omega_\gamma}{m_q}\left(1 + \frac{\omega_\gamma}{2m_q}\right)\boldsymbol{\sigma} \cdot \boldsymbol{\epsilon} + \frac{\omega_\gamma}{\alpha^2}\boldsymbol{\sigma} \cdot \mathbf{A}\boldsymbol{\epsilon} \cdot \mathbf{q}\right]\frac{1}{(n-1)!}\left(\frac{\mathbf{k} \cdot \mathbf{q}}{3\alpha^2}\right)^{n-1}$$

$$+ \frac{\omega_\eta\omega_\gamma}{9\alpha^2 m_q}\boldsymbol{\sigma} \cdot \mathbf{k}\boldsymbol{\epsilon} \cdot \mathbf{q}\frac{1}{(n-2)!}\left(\frac{\mathbf{k} \cdot \mathbf{q}}{3\alpha^2}\right)^{n-2} \tag{24}$$

and

$$\mathcal{O}_n^2 = 0 . \tag{25}$$

Generally, the resonances with large quantum number n become important as the energy increases. Furthermore, the higher partial wave resonances with orbital angular momentum $L = n$ become dominant, which correspond to the resonance $G_{17}(2190)$ for $n = 3$ and $H_{19}(2250)$ for $n = 4$ for η photoproduction. Indeed, only these higher partial wave resonances can be seen experimentally, and

this is consistent with the quark model predictions. Thus we simply take the masses and decay widths of these high partial wave resonances as input in Eq. (16).

III. NUMERICAL EVALUATION

We shall take the same procedure as that in the calculation of kaon photoproduction [1]. In order to take into account of the relativistic effects, the Lorentz boost factor is introduced in the CGLN amplitudes,

$$f_i(\mathbf{k}, \mathbf{q}) \rightarrow \frac{M_N^2}{E_N^i E_N^f} f_i \left(\frac{M_N}{E_N^i}\mathbf{k}, \frac{M_N}{E_N^f}\mathbf{q} \right) , \qquad (26)$$

where $i = 1, ..., 4$ and $M_N/E_N^i (M_N/E_N^f)$ is a Lorentz boost factor for the initial (final) state.

The parameters in this calculation have standard values in the quark model, where the quark mass m_q is 0.34 GeV and $\alpha^2 = 0.16$ GeV^2. The masses and decay widths for the S-channel resonances are taken from the recent particle data group [20]. In principle, there is only one parameter α_η to be determined in the numerical evaluation, in which the wave functions of the resonances are assumed to have SU(6)$\otimes$O(3) symmetry. However, one should not expect that quark model in the SU(6)$\otimes$O(3) symmetry limit could provide a quantitative description of η production, since there should be significant configuration mixing [19]. In particular, the configuration mixing between the states $N(^2P_M)\frac{1}{2}^{-1}$ and $N(^4P_M)\frac{1}{2}^{-1}$ generates a nonzero contribution from the

resonance $S_{11}(1650)$ and thus affects η photoproduction in the threshold region significantly. Evaluations in the potential quark model [19] show that this mixing is indeed very strong. Therefore, we introduce two parameters $C_{S_{11}(1535)}$ and $C_{S_{11}(1650)}$ to take into account configuration mixing effects. The contributions from the resonances $S_{11}(1535)$ and $S_{11}(1650)$ become

$$\mathcal{O}_{S_{11}(1535)} = C_{S_{11}(1535)}\mathcal{O}_{N(^2P_M)\frac{1}{2}^{-1}} \qquad (27)$$

and

$$\mathcal{O}_{S_{11}(1650)} = C_{S_{11}(1650)}\mathcal{O}_{N(^2P_M)\frac{1}{2}^{-1}} , \qquad (28)$$

where $\mathcal{O}_{N(^2P_M)\frac{1}{2}^{-1}}$ is given in Table II. Furthermore, the U-channel contributions given in Eq. (10) represent the result in the SU(6) symmetry limit, which corresponds to $C_{S_{11}(1535)} = 1$ and $C_{S_{11}(1650)} = 0$. There should be an additional U-channel contribution for the general coefficients $C_{S_{11}}$, and it is given by

$$\mathcal{M}_{S_{11}}^U = \frac{-M_{S_{11}}\omega_\gamma e^{-(\mathbf{q}^2+\mathbf{k}^2)/6\alpha^2}}{P_N^f \cdot k + \delta M_{S_{11}}^2/2} \frac{C_{S_{11}(1535)} + C_{S_{11}(1650)} - 1}{3} \left\{ \frac{\mathbf{q}^2}{3\alpha^2} \left[\frac{\omega_\eta}{E_N^f + M_N} + 1 \right] \right.$$
$$\left. - \frac{\omega_\eta}{m_q} + \frac{\mathbf{q} \cdot \mathbf{k}}{3\alpha^2} \left[\frac{\omega_\eta}{E^f + M_N} + \frac{\omega_\eta}{E^i + M_N} \right] \right\} \left(1 + \frac{\omega_\gamma}{2m_q} \right) \boldsymbol{\sigma} \cdot \boldsymbol{\epsilon} , \qquad (29)$$

where $M_{S_{11}(1535)} \approx M_{S_{11}(1650)} \approx 1.6$ GeV in the U channel. In principle, the coefficients $C_{S_{11}}$ could be obtained from the potential quark models that reproduce the baryon spectroscopy. On the other hand, the coefficients $C_{S_{11}}$ obtained from the fitting procedure could provide an important test to the wave functions in the potential quark models. Moreover, whether the quark model could reproduce the large branching ratio for the resonance $S_{11}(1535)$ decaying into the ηN channel is still an open question. Therefore, we adopt two approaches in the numerical evaluation. First, the wave functions of the resonances are assumed to be in the exact symmetry limit; thus, only one parameter α_η is needed to fit the data. Second, we treat the coefficients $C_{S_{11}(1535)}$ and $C_{S_{11}(1650)}$ and the total decay width of the resonance $S_{11}(1535)$, $\Gamma_{S_{11}(1535)}$, as free parameters and fit them to the differential cross section data.

The function minimization routine [24] is used to minimize the least squares function

$$\chi^2 = \sum_i \frac{[X_i - Y_i(a_1, ..., a_n)]^2}{\sigma_{X_i}^2} , \qquad (30)$$

where X_i represents the experimental data, σ_{X_i} corresponds to the error of the data, and $Y_i(a_1, ..., a_n)$ is the theoretical predictions with parameters $a_1, ..., a_n$ to be fitted. There are about 150 points of differential cross section data up to $E_{\text{lab}} = 1.45$ GeV from the old data set [21] and recent data by Homma et al. [22] and by Dytman et al. [6]. More recently, new experimental data in the threshold region from the Mainz group have been published [8]. This set of data differs significantly from

the old set of data [21] and recent Bates data [6] in the threshold region. Therefore, we shall fit the Mainz data separately, and the parameters obtained in these fits are summarized in Table III. Although there are also few target polarization data [23], they will not be used in our fitting because these data have large errors and do not present any systemic behavior on the target polarization.

In fit 1, we assume that the resonances have exact SU(6)$\otimes$O(3) symmetry, and the masses and decay widths of resonances come from the recent particle data group [20]. Therefore, there is only one parameter α_η left to fit the data, and we find

$$\alpha_\eta = 0.465 \qquad (31)$$

by fitting it to combinations of old data [21,22] and recent data from Bates [6]. We present the energy dependence of the differential cross sections at $\theta_{\text{c.m.}} = 50° \pm 5°$ in Fig. 1, at $\theta_{\text{c.m.}} = 90° \pm 8°$ in Fig. 2, and the energy dependence of the total cross section is shown in Fig. 3. Considering that there is only one parameter in the calculation, the overall agreement with the data is truly remarkable. Our calculation in the symmetry limit also

TABLE III. Parameters obtained from different fits. The decay width $\Gamma_{S_{11}(1535)}$ is in units of GeV.

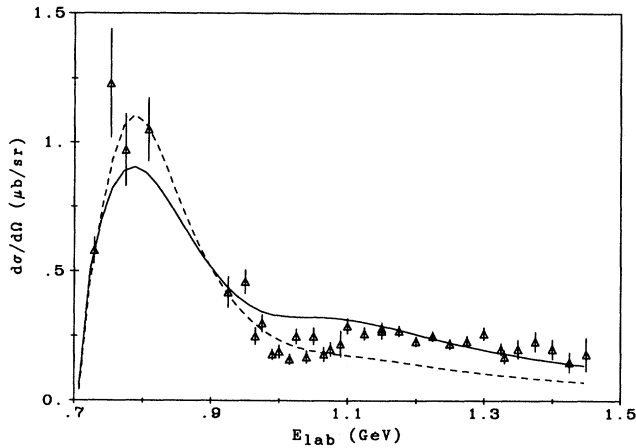|	Fit 1	Fit 2	Fit 3
α_η	0.465	0.139	0.435
$C_{S_{11}(1535)}$	1.0	1.510	1.608
$C_{S_{11}(1650)}$	0.0	−0.036	0.0
$\Gamma_{S_{11}(1535)}$	0.150	0.111	0.198

FIG. 1. Energy dependence of the differential cross section at $\theta_{c.m.} = 50° \pm 5°$. The solid line represents the result from fit 1 and the dashed line from fit 2. The data come from Refs. [21,22,6].

FIG. 3. Energy dependence of the total cross section. The solid is the result from fit 1 and dashed line from fit 2.

shows that the resonance $S_{11}(1535)$ is less dominant than the data suggest, and the calculated total cross section is significantly larger than the data in the $E_{lab} \approx 0.9 - 1$ GeV region. This suggests that the resonance $S_{11}(1650)$ also plays a significant role in addition to the dominant presence of the resonance $S_{11}(1535)$. Therefore, we treat the coupling constant α_η, two coefficients $C_{S_{11}}$, and the decay width $\Gamma_{S_{11}(1535)}$ as a free parameter in fit 2, the resulting parameters are shown in Table III. The resulting fits are also shown in Figs. 1, 2, and 3, respectively. It is worth mentioning that the smaller total decay width $\Gamma_{S_{11}(1535)} = 0.111$ GeV is largely due to the recent Bates data [6] at $E_{lab} = 0.729$ GeV. Since only the differential cross-section data are used in our fits, the recent total cross-section data [7] from ELSA are not used here. Clearly, the threshold region is quite crucial in determining the mass and width of the resonance $S_{11}(1535)$. The resonance $S_{11}(1535)$ becomes more dominant in this fit, and we find a small but negative contribution from the resonance $S_{11}(1650)$. This is qualitatively in agreement
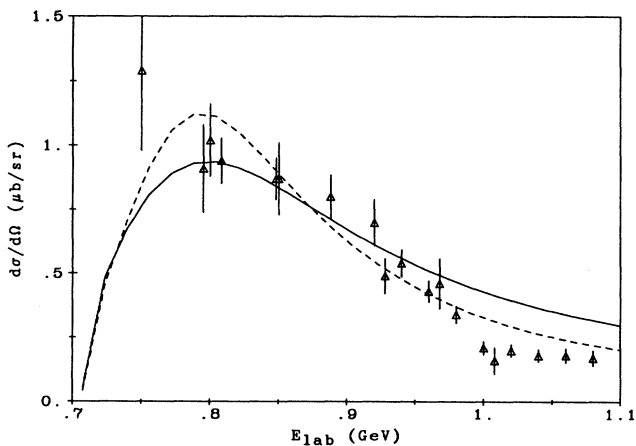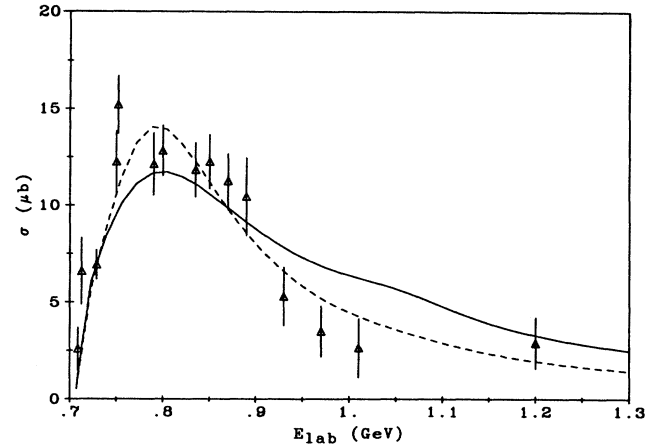

FIG. 2. Same as Fig. 1 at $\theta = 90° \pm 8°$.

with the recent calculation by the RPI group [13], in which the effective Lagrangian approach is used . On the other hand, the coupling constant α_η is significantly reduced from 0.465 to about 0.14; this shows how strongly dependent is the coupling constant α_η on the behavior of the resonances $S_{11}(1535)$ and the resonance $S_{11}(1650)$. The physical reason behind the large reduction of the coupling constant α_η is that the threshold region is dominated by the resonance $S_{11}(1535)$, which accounts for nearly 90% of the total cross section; thus, a small variation in $S_{11}(1535)$ will lead to a larger change in the contribution from the Born term. This shows that the threshold region alone is not a reliable source to determine the ηNN coupling constant α_η.

In fit 3, we are concentrating on the recent published data from the Mainz group [8], in which more systematic differential cross section data are presented from $E_{lab} = 0.716$ to 0.788 GeV. It should be pointed out that these data are significantly larger than the previous data in threshold region [21,6,22]; therefore, further experimental confirmation is needed. Because this set of data is concentrated on the region from the threshold to the mass of the resonance $S_{11}(1535)$, one could not obtain any reliable information on the contribution from the resonance $S_{11}(1650)$. Thus we exclude the contribution from the resonance $S_{11}(1650)$ by setting the parameter $C_{S_{11}(1650)} = 0.0$, which is the same as that in fit 1. Thus three parameters α_η, $C_{S_{11}(1535)}$, and $\Gamma_{S_{11}(1535)}$ are fitted to the data. The calculated total cross section and the data are presented in Fig. 4, and the agreement with the data is excellent. Moreover, the resulting decay width $\Gamma_{S_{11}(1535)}$ is found to be 0.198 GeV and in very good agreement with the simple Breit-Wigner fit [8]. This provides an important consistency check of the model. One could also see the possible contribution from the resonance $S_{11}(1650)$ at $E_{lab} \approx 0.8$ GeV, where the data suggest that the total cross section starts to decrease. More systematic data in $E_{lab} = 0.8 - 1.0$ GeV region are needed in order to learn more about the structure of both $S_{11}(1535)$ and $S_{11}(1650)$.
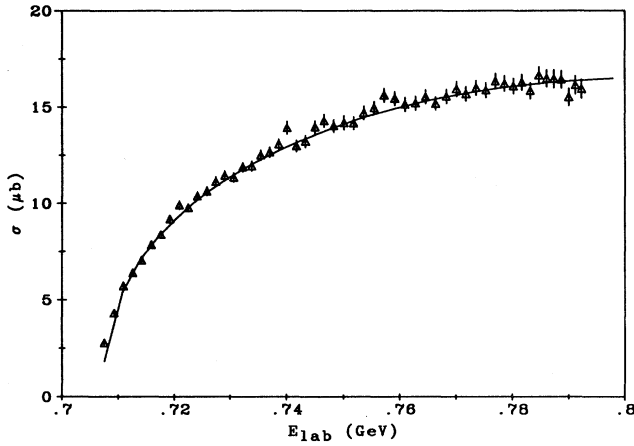
To highlight the importance of the data in the thresh-

FIG. 4. Result for the total cross section from fit 3, in which the parameters are fitted to the data from Mainz [8].

FIG. 6. Same as Fig. 4 at $E_{lab} = 0.752$ GeV.

old region in determining the properties of the resonance $S_{11}(1535)$ and coupling constant α_η, we show the differential cross section at $E_{lab} = 0.729$ GeV in Fig. 5 and $E_{lab} = 0.752$ in Fig. 6. Notice that there is a significant difference between the data from Bates [6] and Mainz [8] at $E_{lab} = 0.729$ GeV; it leads to the change from $\Gamma_{S_{11}(1535)} = 0.111$ GeV in fit 2 to 0.198 GeV in fit 3. Resolving this difference in the future experiments is crucial for understanding the structure of the resonance $S_{11}(1535)$. At the same time, the parameter α_η is changed by a factor of 3. In fact, the calculation by the RPI group [13] has shown that one could obtain a good fit to the data in the threshold region for a wide range of coupling constant α_η. More systematic data beyond the threshold region are called for, particularly in the region $E_{lab} = 1.15 - 1.45$ GeV, in which there is no resonance dominant so that contribution from the Born term becomes relatively important. It is interesting to note that the calculated differential cross section in fit 2 is in good
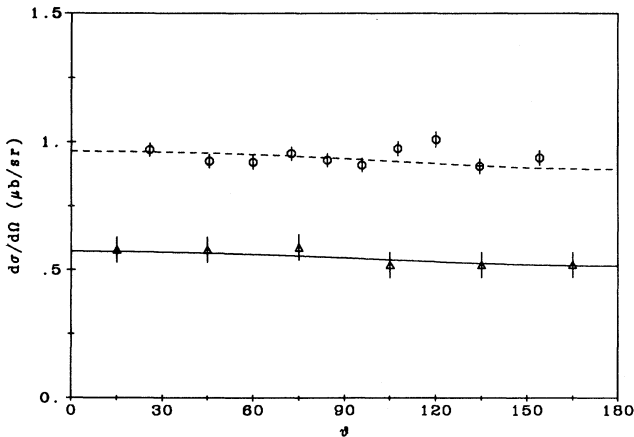
agreement with the Bate data [6] at $E_{lab} = 0.729$ GeV, but smaller at $E_{lab} = 0.752$ GeV, while the results in fit 3 give excellent fits to the Mainz data [8] in both cases.

We should also point out that the resonances $P_{11}(1710)$ and $P_{13}(1720)$ also play quite important role in the region $E_{lab} = 0.9 - 1.1$ GeV, and one should not expect that the quark model in the symmetry limit would provide a quantitative description of these resonances. One could also study these resonances by inserting coefficients in front of their CGLN amplitudes and fitting them to the data. Our calculation provides a framework to study the resonance contributions in meson photoproduction with less parameters. This will be investigated in the future with more accurate data in this region.

The calculation of the target polarizability has also been done with the parameters in each fit. We found consistent small polarizabilities at $\theta_{c.m.} = 90°$ from the threshold to $E_{lab} = 1.0$ GeV. If the polarization is indeed large in this region as the data suggest [23], it might be evidence that t-channel meson exchange is required.

FIG. 5. Differential cross section at $E_{lab} = 0.729$ GeV. The solid line represents the result from fit 2 and dashed line from fit 3. The data come from Ref. [6] (triangle) and Ref. [8] (circle).
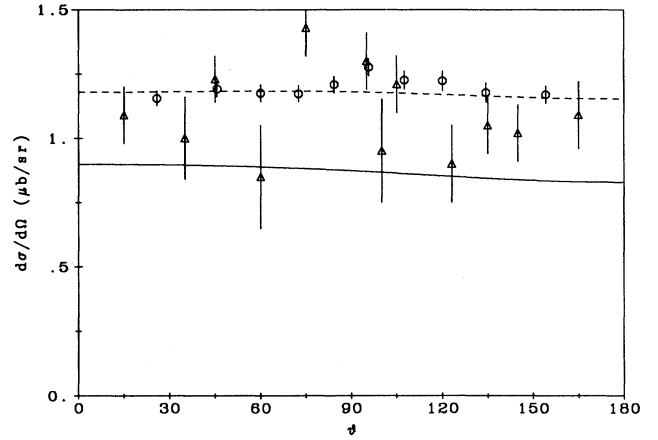
IV. STRUCTURE OF THE RESONANCE $S_{11}(1535)$

There were probably two important motivations to study η photoproduction in the threshold region: to determine the ηNN coupling constant α_η and to study the structure of the resonance $S_{11}(1535)$. Our calculation shows that the threshold region might not be a reliable source to determine the coupling constant α_η because of the dominance of the resonance $S_{11}(1535)$. However, one might be able to learn more about the structure of the resonance $S_{11}(1535)$ in the quark model. The study [13] by the RPI group shows that one could determine the quantity ξ from η photoproduction, which is defined as

$$\xi = \sqrt{\chi' \Gamma_\eta} A_{1/2}/\Gamma_T , \qquad (32)$$

where $\chi' = M_N k/q M_R$. One can obtain an analytic expression of the quantity ξ from the CGLN amplitude in Table II, which is given by

$$\xi = \sqrt{\frac{\alpha_\eta \alpha_e \pi (E^f + M_N)}{M_R^3} \frac{C_{S_{11}(1535)}\omega_\gamma}{6\Gamma_T}} \left[\frac{2\omega_\eta}{m_q} - \frac{2\mathbf{q}^2}{3\alpha^2} \left(\frac{\omega_\eta}{E^f + M_N} + 1 \right) \right] \left(1 + \frac{|\mathbf{k}|}{2m_q} \right) e^{-(\mathbf{q}^2 + \mathbf{k}^2)/6\alpha^2} . \tag{33}$$

Because $\mathbf{q}^2 \ll 1$, the quantity ξ for the resonance $S_{11}(1535)$ is not sensitive to the parameter α^2 related to the internal structure of the baryon wave functions. After including the Lorentz boost factors in Eq. (26), we obtain

$$\xi = \begin{cases} 0.186 & \text{from fit 1} , \\ 0.208 & \text{from fit 2} , \\ 0.220 & \text{from fit 3} , \end{cases} \tag{34}$$

in units of GeV^{-1}. This is indeed in good agreement with the result $\xi = 0.22 \pm 0.02$ GeV^{-1} in Ref. [13]. It is not surprising that the quantity ξ in fit 1 is smaller, because the resonance $S_{11}(1535)$ is less dominant in the symmetry limit than the data suggested. Therefore, assuming that the branching ration for the resonance $S_{11}(1535) \to \eta N$ is around 0.5, we have the helicity amplitude

$$A_{1/2}^p = \begin{cases} 81 & \text{from fit 1} , \\ 78 & \text{from fit 2} , \\ 111 & \text{from fit 3} , \end{cases} \tag{35}$$

in units of 10^{-3} GeV$^{-1/2}$, which is very consistent with the results of Ref. [13] in fits 1 and 2 and of Ref. [8] in fit 3.

The advantage of the quark model calculation is that the helicity amplitude $A_{1/2}^p$ and the decay width $\Gamma_{S_{11}(1535)}$ can be predicted separately. In the symmetry limit, the helicity amplitude $A_{1/2}^p$ is given by [26]

$$A_{1/2}^p = \sqrt{2\alpha_e \pi \omega_\gamma} \frac{1}{3\alpha} \left(1 + \frac{|\mathbf{k}|}{2m_q} \right) e^{-\mathbf{k}^2/6\alpha^2} , \tag{36}$$

and the decay width in the $S_{11}(1535) \to \eta N$ channel is expressed in terms of the coupling constant α_η:

$$\Gamma_{S_{11}(1535)}(\eta N) = \frac{\alpha_\eta (E + M_N)|\mathbf{q}|}{2M_R} \frac{\alpha^2}{M_N^2}$$
$$\times \left\{ \frac{\omega_\eta}{m_q} - \frac{\mathbf{q}^2}{3\alpha^2} \left[\frac{\omega_\eta}{E + M_N} + 1 \right] \right\}^2$$
$$\times e^{-\mathbf{q}^2/3\alpha^2} . \tag{37}$$

We have

$$A_{1/2}^p = 148 \times 10^{-3} \text{ GeV}^{-1/2} \tag{38}$$

and

$$\Gamma_{S_{11}(1535)}(\eta N) = 23.4 \text{ MeV} \tag{39}$$

after including the Lorentz boost factors. Comparing this prediction with the results in fit 1, the helicity amplitude $A_{1/2}^p$ predicted by the quark is twice as large as the data, while the decay width is about a factor of 3 smaller. The fact that there is a factor of 2 between the old data and the quark model calculations for the helic-

ity amplitude $A_{1/2}^p$ has been known for some time [10,9], and it was speculated that this might be an indication of configuration mixing [25]. However, systematic calculations with the configuration mixings in the Isgur-Karl model showed [26] that the configuration mixing effects are unable to reduce the helicity amplitude $A_{1/2}^p$. Therefore, it is particularly interesting that the new data set from Mainz has brought the helicity amplitude $A_{1/2}^p$ in fit 3 much closer to the quark model predictions; the simple Breit-Wigner fit in Ref. [8] also gives

$$A_{1/2}^p = (125 \pm 25) \times 10^{-3} \text{ GeV}^{-1/2} , \tag{40}$$

which is even closer to the quark model result in Eq. (38).

On the other hand, the large ηN branching ratio for the resonance $S_{11}(1535)$ has not been fully understood. The calculation by Koniuk and Isgur [10] also shows that the transition amplitude for $S_{11}(1535) \to \eta N$ is about 50% smaller than the data, whose calculation is similar to this approach. This is consistent with the fitted coefficient $C_{S_{11}(1535)} \approx 1.5$ in both fits 2 and 3, and it is unlikely that this can be explained by configuration mixing effects. One of the effects that has not been taken into account in this study is the finite size of η mesons, which is the one of the major motivations of the quark pair creation model [27]. The calculation has been partly done in Ref. [28], which gives a much larger decay amplitude. The problem is that the ηNN coupling that can also be obtained in this approach was not given; thus, there is no basis to judge if the parameter used in the calculation is reasonable.

The understanding of the ηN branching ratio of the resonance $S_{11}(1535)$ may be the key to its underlying structure. It has been discussed for some time in the literature that the resonance $\Lambda(1409)$ might be a kaon-nucleon binding state, whose mass is just below the kaon-nucleon threshold. Notice that the mass of the resonance $S_{11}(1535)$ is just below the threshold of kaon production, $\gamma N \to K\Lambda$ and $\gamma N \to K\Sigma$; it would be interesting to study the possibility that the resonance $S_{11}(1535)$ is a combination of q^3 and $K\Lambda$ or $K\Sigma$ binding states, which suggests that the state $\Lambda(1409)$ as a KN binding state might not be an isolated case. The threshold behavior of kaon photoproduction, $\gamma N \to K\Lambda$ and $\gamma N \to K\Sigma$, may provide us further information in this regard, because it is dominated by S-wave resonances and the Born terms.

V. CONCLUSIONS

The first quark model calculation is presented for η photoproduction, which provides a very good description of η photoproduction with fewer parameters. We show that the threshold region is not a reliable place to determine the ηNN coupling constant, which strongly

depends on the properties of the resonance $S_{11}(1535)$. One should extend that study to $E_{lab} = 1.4$ GeV region, in which no resonance is dominant, so that the contribution from the Born term could be determined more reliably. If there is any indication from the recent Mainz data, it might be that the old set of data may become irrelevant. Certainly, future experiments planned at various facilities, in particular at the Continuous Electron Beam Accelerator Facility (CEBAF), will provide us much more accurate information on η photoproduction that will reach beyond the threshold region. The results here show that the quark model approach will certainly be a very effective tool for studying the underlying structure of baryon resonances from the photoproduction data.

ACKNOWLEDGMENTS

[1] Zhenping Li, Phys. Rev. C **52**, 1648 (1995).

[2] A. Manohar and H. Georgi, Nucl. Phys. **B234**, 189 (1984).

[3] G. F. Chew, M. L. Goldberger, F. E. Low, and Y. Nambu, Phys. Rev. **106**, 1345 (1957); S. Fubini, G. Furlan, and C. Rossetti, Nuovo Cimento **40**, 1171 (1965).

[4] Zhenping Li, Phys. Rev. D **50**, 5639 (1994).

[5] Zhenping Li, Phys. Rev. D **48**, 3070 (1993).

[6] S. Dytman *et al.*, Phys. Rev. C **51**, 2170 (1995).

[7] J. Price *et al.*, Phys. Rev. C **51**, R2283 (1995).

[8] B. Krusche *et al.*, Phys. Rev. Lett. **74**, 3736 (1995).

[9] F. E. Close and Zhenping Li, Phys. Rev D **42**, 2194 (1990).

[10] R. Koniuk and N. Isgur, Phys. Rev. D **21**, 1888 (1980).

[11] H. R. Hicks *et al.*, Phys. Rev. D **7**, 2614 (1973), and references therein.

[12] C. Bennhold and H. Tanabe, Phys. Lett. B **243**, 12 (1990).

[13] M. Benmerrouche, N. C. Mukhopadhyay, and J. F. Zhang, Phys. Rev. D **51**, 3237 (1995); M. Benmerrouche and N. Mukhopadhyay, Phys. Rev. Lett. **67**, 101 (1992).

[14] C. G. Fasano, F. Tabakin, and B. Saghai, Phys. Rev. C **46**, 2430 (1992).

[15] R. Dolen, D. Horn, and C. Schmid, Phys. Rev. **166**, 1768 (1966).

[16] J. M. Blatt and V. F. Weisskopf, *Theoretical Nuclear Physics* (Wiley, New York, 1952), p. 361.

[17] Zhenping Li, M. Guidry, T. Barnes, and E. S. Swanson, MIT-ORNL Report No. MIT-CTP-2277/ORNL-CCIP-94-01 (unpublished).

[18] R. G. Moorhouse, Phys. Rev. Lett. **16**, 772 (1966).

[19] N. Isgur and G. Karl, Phys. Rev. D **18**, 4187 (1978); **19**, 2194 (1979).

[20] Particle Data Group, L. Montanet *et al.*, Phys. Rev. D **50**, 1173 (1994).

[21] H. Genzel, P. Joos, and W. Pfeil, in *Landolt-Börstein*, edited by H. Genzel, P. Joos, and W. Pfeil, New Series, I/8 (Springer, New York, 1973), p. 278.

[22] S. Homma *et al.*, J. Phys. Soc. Jpn. **57**, 1381 (1988).

[23] C. A. Heusch *et al.*, Phys. Rev. Lett. **25**, 1381 (1970).

[24] W. H. Press *et al.*, *Numerical Recipes* (Cambridge University Press, New York, 1986), p. 289.

[25] F. Foster and G. Hughes, Z. Phys. C **14**, 123 (1982).

[26] Zhenping Li and F. E. Close, Phys. Rev. D **42**, 2207 (1990).

[27] Le Yaouanc *et al.*, *Hadron Transitions in the Quark Model* (Gordon and Breach, New York, 1988); Phys. Rev. D **8**, 2223 (1973); **9**, 1415 (1974).

[28] S. Capstick and W. Roberts, Phys. Rev. D **49**, 4570 (1994).